

Supplementary material

Electrochemical response of a COF/MWCNT sensor based on a bifunctional COF towards dopamine and uric acid

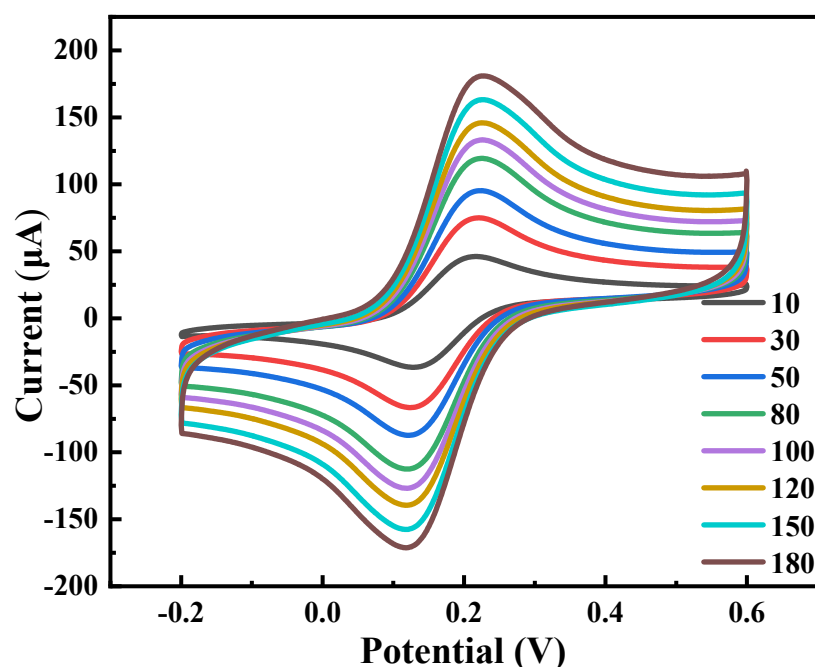


Fig. S1 CV curves of the COF/MWCNT/GCE electrode at various scan rates in $[\text{Fe}(\text{CN})_6]^{3-/4-}$ solution

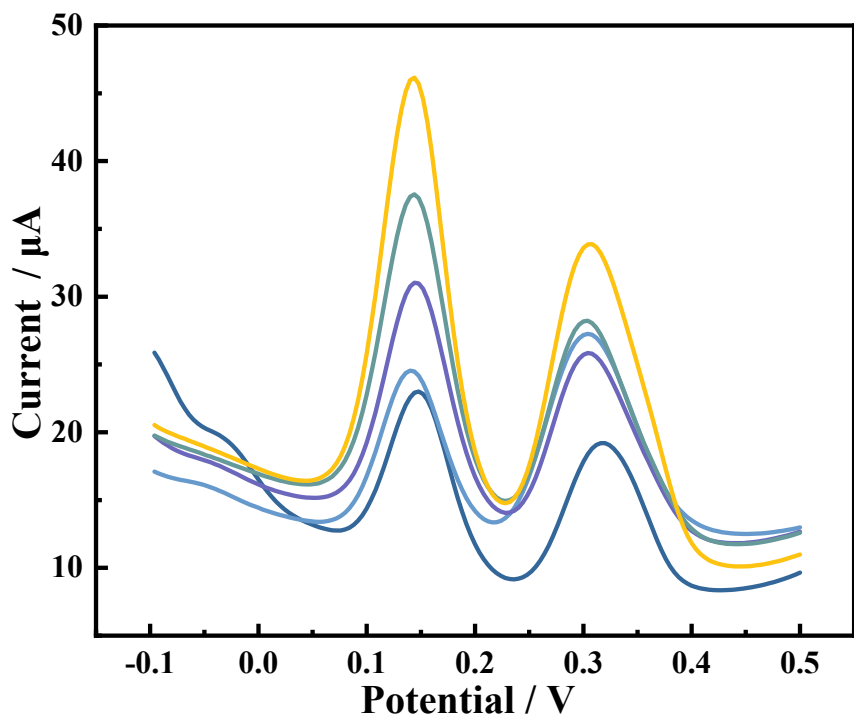


Fig. S2 Response of electrochemical sensors prepared under different concentration conditions to DA and UA

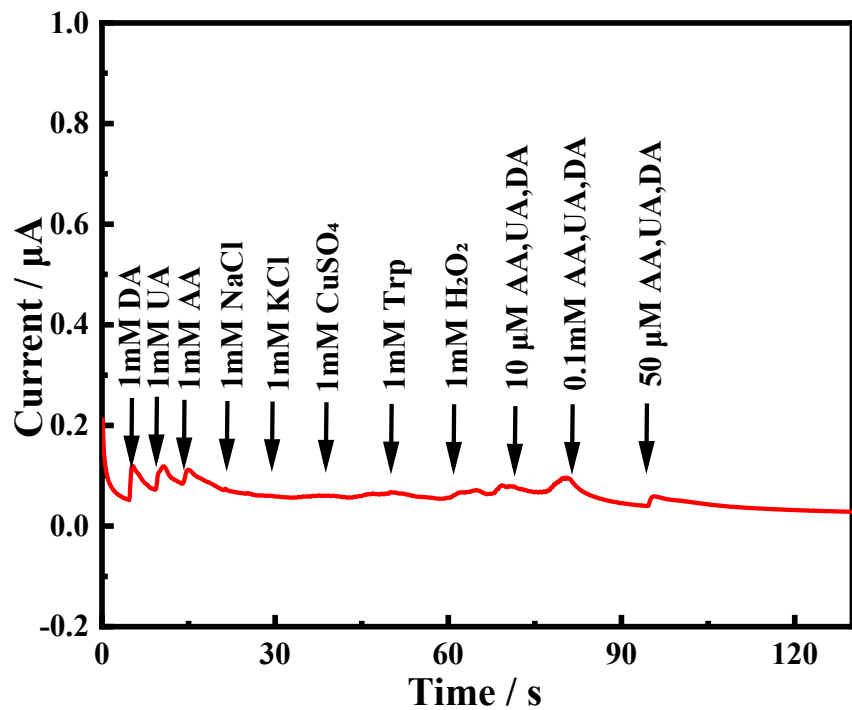


Fig. S3 Anti-interference ability of COF/MWCNT/GCE

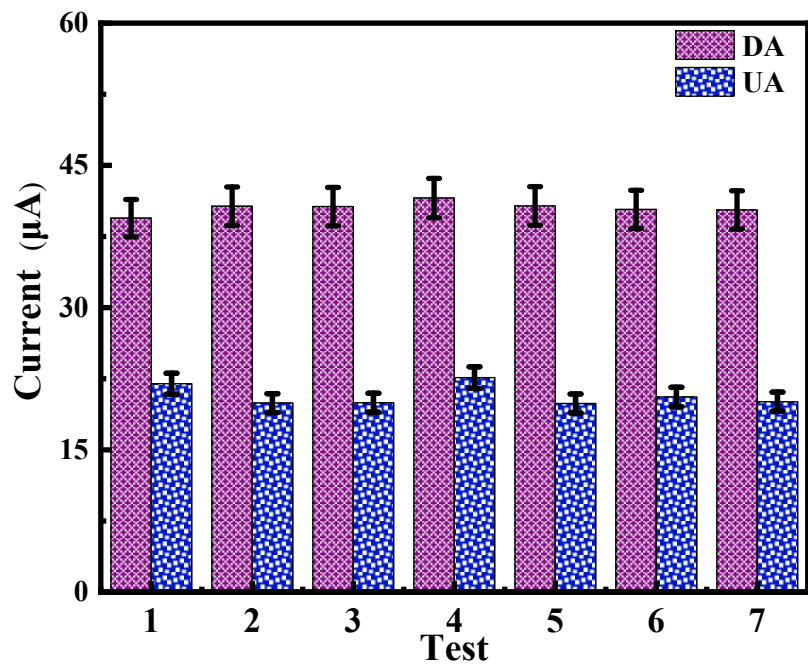


Fig. S4 Stability of COF/MWCNT/GCE (DA and UA concentrations were both 100 μM)

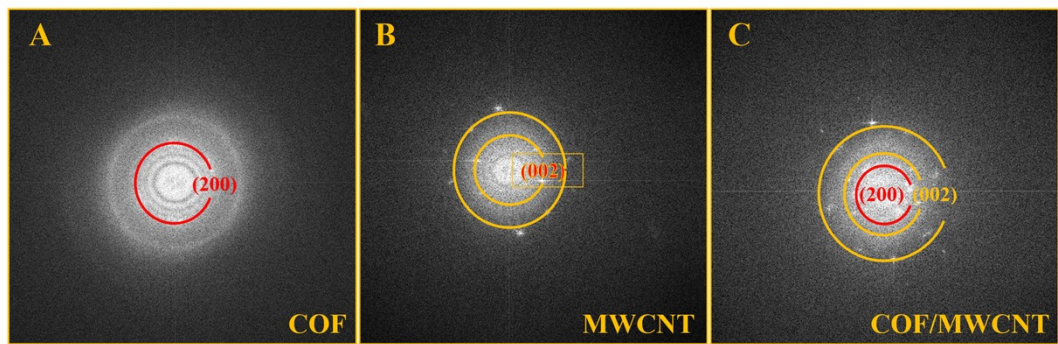


Fig. S5 SAED patterns of COF(A), MWCNT(B), and COF/MWCNT(C)

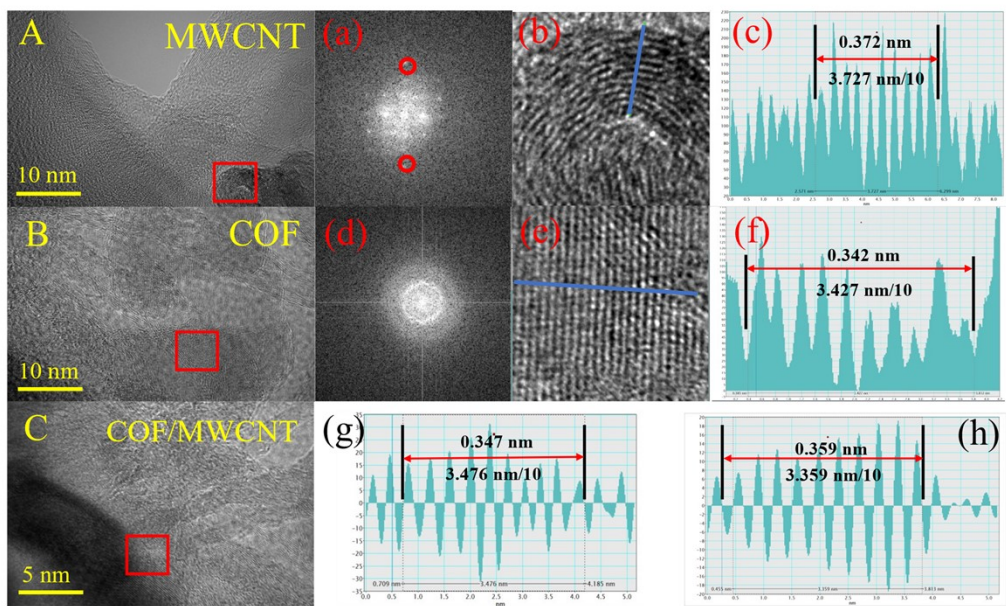


Fig. S6 The spacing of stripes for different substances in TEM

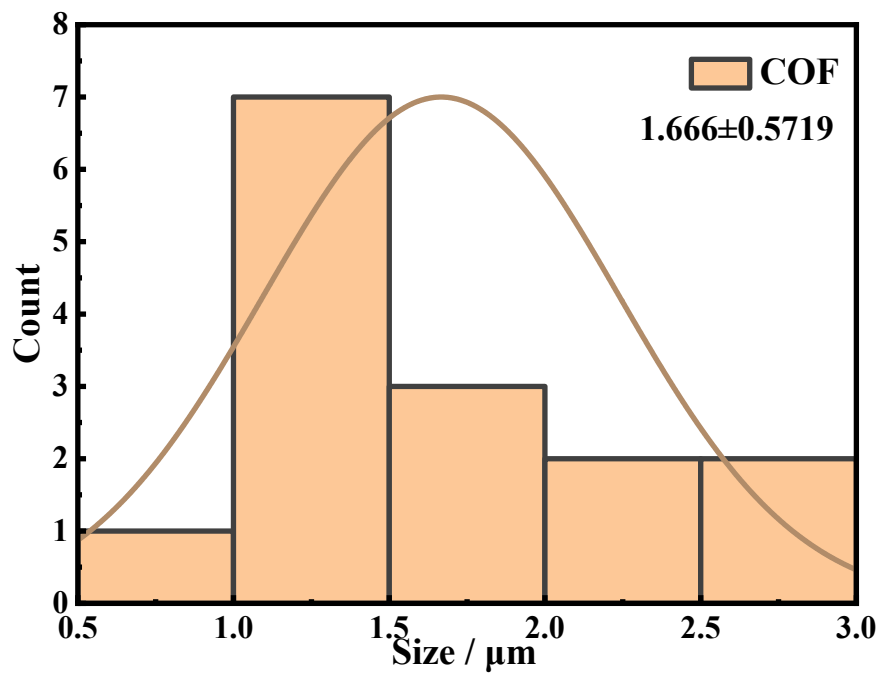


Fig. S7 Particle size distribution of COF materials

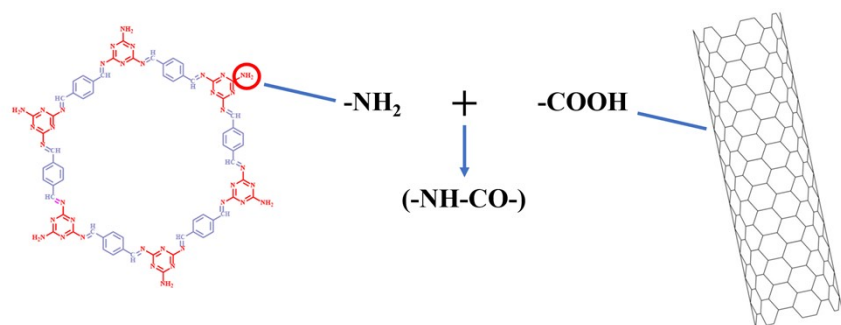
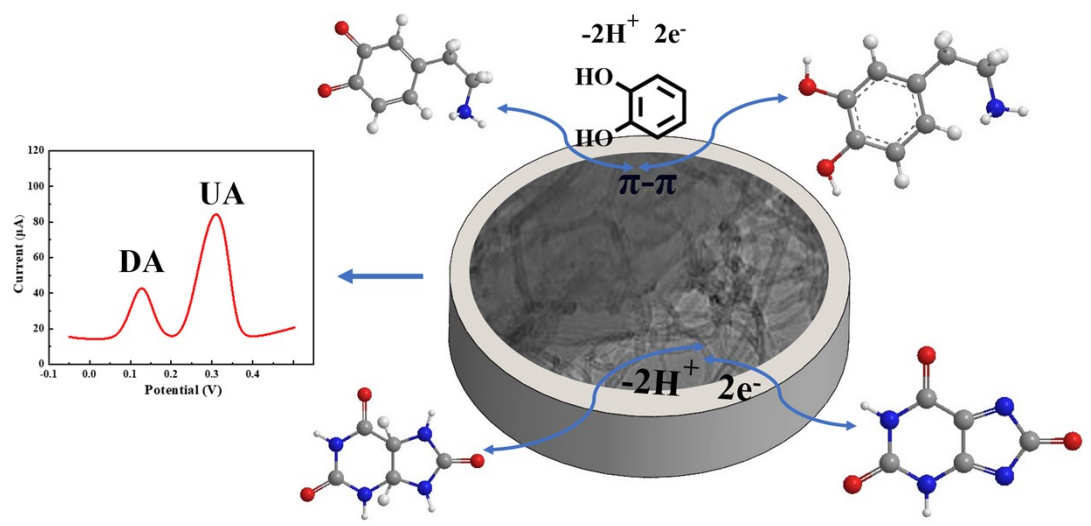


Fig. S8 Chemical interactions between COF and MWCNT



Scheme S1 The interaction between dopamine, uric acid, and the COF/MWCNT composite

Table S1 Selectivity recovery rates

Chaff interferent	Concentration (μM)	DA (%)	RSD (%)	UA (%)	RSD (%)	HPLC
AA	500	98.2	2.8	97.6	3.2	99.1
KCl	1000	102.4	3.1	96.3	2.9	101.3
H_2O_2	2000	95.7	2.4	94.8	2.7	96.5
NaCl	10 mM	103.1	3.5	101.5	3.8	104.2

Table S2 Electrode stability test

Test	DA (μA)	Error bar %	UA (μA)	Error bar %
1	20.22	1.969	39.38	1.011
2	18.94	1.9885	39.77	0.947
3	20.46	2.099	41.98	1.023
4	20.22	2.1275	42.55	1.011
5	19.65	2.0805	41.61	0.9825
6	19.65	2.063	41.26	0.9825
7	18.61	2.056	41.12	0.9305

Table S3 Results of DA recovery detection in urine samples

Samples	Addition (μM)	Recovery (μM)	Recovery (%)	RSD (%)
1	10	9.45	94.50	4.38
2	500	520.33	104.07	4.73
3	1000	942.51	94.25	4.14

Table S4 Results of DA recovery detection in urine samples

Samples	Addition (μM)	Recovery (μM)	Recovery (%)	RSD (%)
1	20	20.51	102.55	2.7
2	200	193.55	96.77	1.26
3	2000	2115.66	105.78	1.64